Lateral shearing interferometry, dynamic wavefront sensing, and high-speed videokeratoscopy for noninvasive assessment of tear film surface characteristics: a comparative study

Dorota H. Szczesna
Wroclaw University of Technology
Institute of Physics
27 Wybrzeze Wyspianskiego
Wroclaw, 50-370 Poland
and
Queensland University of Technology
School of Optometry
Victoria Park Road
Kelvin Grove Brisbane, QLD 4059
Australia

David Alonso-Caneiro
D. Robert Iskander
Scott A. Read
Michael J. Collins
Queensland University of Technology
School of Optometry
Victoria Park Road
Kelvin Grove Brisbane, QLD 4059
Australia

Abstract. There are several noninvasive techniques for assessing the kinetics of tear film, but no comparative studies have been conducted to evaluate their efficacies. Our aim is to test and compare techniques based on high-speed videokeratoscopy (HSV), dynamic wavefront sensing (DWS), and lateral shearing interferometry (LSI). Algorithms are developed to estimate the tear film build-up time T_{BLD}, and the average tear film surface quality in the stable phase of the interblink interval $TFSQ_{Av}$. Moderate but significant correlations are found between T_{BLD} measured with LSI and DWS based on vertical coma (Pearson's $r^2=0.34$, $p<0.01$) and higher order rms ($r^2=0.31$, $p<0.01$), as well as between $TFSQ_{Av}$ measured with LSI and HSV ($r^2=0.35$, $p<0.01$), and between LSI and DWS based on the rms fit error ($r^2=0.40$, $p<0.01$). No significant correlation is found between HSV and DWS. All three techniques estimate tear film build-up time to be below 2.5 sec, and they achieve a remarkably close median value of 0.7 sec. HSV appears to be the most precise method for measuring tear film surface quality. LSI appears to be the most sensitive method for analyzing tear film build-up. [DOI: 10.1117/1.3431103]

Keywords: tear film kinetics; videokeratoscopy; wavefront sensing; interferometry.

Paper 09483RR received Nov. 4, 2009; revised manuscript received Mar. 15, 2010; accepted for publication Mar. 16, 2010; published online Jun. 9, 2010.

1 Introduction

Evaluating the quality and stability of the tear film is a key clinical task in the diagnosis and management of dry eye. However, many of the available clinical methods for tear film evaluation can be invasive or semi-invasive, rely on subjective judgments, can be time consuming, and unreliable.[1] These shortcomings in traditional clinical tests suggest a need for the development of new methods that are noninvasive, simple to perform, and provide objective quantitative measures of tear film quality and kinetics.[2] Noninvasive methods for assessing the tear film are defined here as methods in which no substance is instilled into the eye, there is no forced blinking or forcible holding of the eyelids, and there is no contact between the measuring instrument and the eye or eyelids. Such noninvasive methods include techniques based on observing changes in the specular reflection of a grid pattern projected on the cornea,[3–8] observing changes in measured wavefront aberrations,[9–12] and those based on observing changes in lateral shearing interferometric patterns.[13–15]

Taking a series of measurements or recording a video in each of these noninvasive techniques enables evaluation of the temporal changes of the tear film surface, and can allow derivation of a time-series-based tear film surface quality (TFSQ) indicator. Then, such an indicator can be used to assess several clinically relevant parameters such as tear film build-up time, a parameter closely related to the spread of the lipid layer,[16,17] the average tear film surface quality in the interblink interval, tear film velocity (the rate of tear flow over time), and may also be used to predict tear film break-up time.

In high-speed videokeratoscopy, changes in corneal topography estimates[5,18] or changes in the quality of videokeratoscopic images[7,19] can be used to infer changes in tear film surface quality. In wavefront sensing, changes in higher-order aberrations (particularly in vertical coma) can be thought as originating from changes in the tear film surface.[10–12] Finally, the assessment of the tear film surface quality in lateral shearing interferometry is essentially based on the first-order frequency estimates of the interference fringes.[14] There are several obvious advantages and disadvantages of each of the three considered noninvasive techniques. Among them, the modified lateral shearing interferometry technique appears to be the most sensitive way of recording tear film surface irregularities.[14] At the same time, the technique is hindered by the natural microfluctuations of the eye, resulting in significant measurement noise.[13] The technique is usually limited to

Address all correspondence to: Dorota H. Szczesna, Wroclaw University of Technology, Institute of Physics, 27 Wybrzeze Wyspianskiego, Wroclaw, 50-370 Poland. Tel: 48-71-320-2592; E-mail: dorota.szczesna@pwr.wroc.pl

1083-3668/2010/15(3)/037005/9/$25.00 © 2010 SPIE

an analysis area of approximately 4×4-mm square, unless large optical elements with high numerical apertures are used. Wavefront sensing provides a very sensitive and accurate assessment of the eye's optics. However, temporal changes in ocular wavefront aberrations can be related to cardiopulmonary signals.[20,21] Wavefront-sensing-based evaluation of tear film surface quality is also limited to the exit pupil area. Finally, high-speed videokeratoscopy with Placido disks may have less spatial resolution than the previous two methods, but it provides maximum surface coverage, encompassing the entire visible corneal surface for analysis.[19]

Our aim in this study was to perform a comparative study of the three considered techniques by conducting measurements of tear film surface kinetics on a cohort of healthy subjects with no evidence of any tear film abnormalities. Two parameters were of particular interest, the tear film build-up time and the average tear film surface quality in the stable phase of the interblink interval.

2 Materials and Methods

2.1 *Subjects*

Right eyes from 18 Caucasian subjects, nine females and nine males, aged from 20 to 57 years were measured in this study. The mean age of all subjects was 32 ± 10 years. None of the subjects were using ocular or systemic medications and none were contact lens wearers. No subject reported any history of significant ocular pathology, injury, or surgery. The study was approved by the university research ethics committee, and all subjects gave informed consent before participation and were treated in accordance with the Declaration of Helsinki.

All subjects were clinically assessed as having a tear film quality within normal limits with no evidence of ocular pathology. The clinical assessment included clinical history, slit lamp examination, phenol red thread test of tear volume, and fluorescein tear film break-up time (FTBUT). The slit lamp assessment included examination of the lid margins and meibomian glands, the bulbar and tarsal conjunctiva, and staining of the ocular surface with fluorescein and lissamine green dye. The central lower tear meniscus height was measured with a slit lamp graticule. All subjects recorded a phenol red thread wetted length of greater than 10 mm. Three measurements of FTBUT were conducted and the average was taken. Fluorescein staining of the cornea and lissamine green staining of the bulbar conjunctiva were graded according to the National Eye Institute (NEI) grading scale.[22] All subjects exhibited corneal and conjunctival staining scores of less than 3. The group average statistics of the clinical measurements, including the mean, standard deviation, median, and the median average distance (MAD), are shown in Table 1.

2.2 *Measurement Protocol*

For each of the subjects, all measurements were taken in the afternoon within a two-hour time frame between 3 and 5 pm. To ensure that the room environmental conditions did not significantly affect tear film quality, all three instruments were located in the same room (see Fig. 1). Temperature and humidity of the room were controlled and recorded at the beginning of each measurement session. The average (mean $\pm$ SD) temperature in the measurement room was (23 ± 1 °C) and the average humidity was (53 ± 5%).

Table 1 Group average statistics of the objective clinical measurements.

	Mean	Std	Median	MAD
Phenol thread wet length (mm)	23.3	6.5	24.0	5.3
FTBUT (seconds)	15.9	13.6	11.0	7.3
Corneal (fluorescein) stain score (0 to 15)	1.03	0.67	1.0	0.54
Conjunctival (lissamine green) stain score (0 to 18)	0.47	0.55	0.25	0.47
Tear meniscus height (mm)	0.26	0.06	0.27	0.05

Due to the need to save large amounts of digital data, the order of use of the instruments was standardized to optimize time management and reduce subject fatigue. Two measurements were taken with each instrument in the following order: high-speed videokeratoscopy (HSV), followed by dynamic wavefront sensing (DWS), and finally lateral shearing interferometry (LSI). During the measurements, subjects were asked to focus on the instrument's fixation target and blink as naturally as possible without deliberately keeping their eyes open during a 30-sec measurement period. A break of about 60 sec was allowed for the subject before a further 30-sec measurement was taken. Data were excluded from analysis if there was obvious reflex tearing and significant eye movements during measurements (i.e., subject not focusing on the target). These decisions were made by an experimenter who was masked to the clinical tear analysis results. Five subjects out of the initially enrolled 23 subjects were excluded from further analysis.

2.3 *Instrumentation*

For completeness, a short summary of the technical aspects of each of the three procedures is given. However, greater detail of each of the procedures can be found in the work of Alonso-Caneiro, Iskander, and Collins for HSV,[19] in the works of

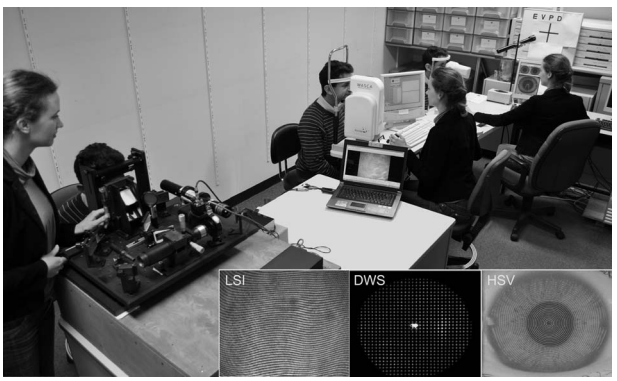

Fig. 1 Measurement setup (a collage). From left: lateral-shearing interferometer (LSI), dynamic wavefront sensor (DWS), and high-speed videokeratoscope (HSV). Insets show examples of video frames from each of the instruments. Measurements were conducted in the following sequence: HSV⇒DWS⇒LSI.

Iskander et al. and Zhu et al. for the DWS technique,[20,21] and in the works of Szczesna et al. and Szczesna and Iskander for LSI.[14,23]

The HSV and LSI techniques captured images at a constant rate of 25 Hz, while the DWS provided sampling frequencies that fluctuated around 7.5 Hz. For each of the methods, blinks were automatically detected in the image sequences, and each sequence was divided into a series of interblink intervals.

During recordings, the eye undergoes natural micromovements,[24] which represent an interference that needs to be detected, because it can cause motion-related blur of the images. This effect is particularly evident in the HSV and LSI measurements. Hence, algorithms were developed to detect the images affected by the blur motion. Such blurred images were subsequently excluded from the analysis in both methods.

2.3.1 *High-speed videokeratoscopy*

The image processing technique from HSV recording operates on the set of images within the interblink interval and involves the following steps.[19] First, estimation of the region of interest is performed. Once the region with the fundamental information is extracted, the next step is to detect the unaltered ring pattern within this area. The technique separates the parts of the image that present a well-structured Placido disk pattern from the interference. After this, the interference is further clustered into two types, depending on the cause. Once the interference from eyelashes has been removed, the remaining interference is assumed to be related to the poor quality tear film.

Finally, tear film surface quality is estimated in the area of analysis (AOA), formed by the area related to the unaltered videokeratoscopy pattern signal and tear disturbance interference. The tear film surface quality indicator is estimated by using the method of image coherence analysis, in which the value of this indicator for each image is the average of the coherence measurement across the area of analysis.[19] Examples of tear film surface quality kinetics estimated within the area of analysis $TFSQ_{AOA}$, and within the pupil area, $TFSQ_{pupil}$, are shown in Fig. 2. The pupil area was used for comparison with the DWS and the LSI techniques that are limited to measuring this region of the ocular surface.

2.3.2 *Dynamic wavefront sensing*

The Complete Ophthalmic Analysis System (COAS™, Wave-Front Sciences, Incorporated) was used for dynamic wavefront sensing. Measurements were performed in a multifile mode. Sampling instabilities are taken into account in the analysis by registering the exact time stamp of each single measurement. Since natural blinking occurred during data acquisition, a procedure for detecting the blinks in the original Hartmann-Shack images was used.

The remaining Hartman-Shack images were used to estimate the wavefront aberrations that were decomposed into Zernike terms, up to and including the eighth radial order, resulting in 45 time-varying coefficients. For this, the instrument's own modal Zernike polynomial fitting algorithm was used. Finally, time series of total, higher-order, comatic terms, and the Zernike polynomial rms fit error were used as possible indicators of tear film surface quality.[10–12,18,25]

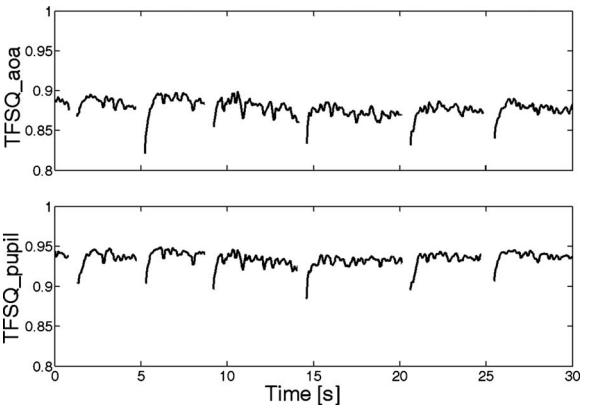

Fig. 2 Examples of the tear film surface quality (TFSQ) dynamics recorded with HSV within the area of analysis (top) of approximately 78 $(mm)^2$ and within the pupil area (bottom) of approximately 38 $(mm)^2$, in which the tear film build-up phase is clearly visible. Gaps in the records indicate the location of blinks that were removed from the dataset.

Wavefront aberrations are also affected by the variations in pupil size, and since the time-varying Zernike polynomial coefficients are calculated for a given pupil size, it is necessary to rescale such coefficient values to a common pupil size.[26] Wavefront aberrations were rescaled to the smallest common pupil diameter in each of the recordings. Examples of wavefront dynamics are shown in Fig. 3, where the time series of total aberrations (TAs), higher-order aberrations (HOA), total comatic terms ($Coma_V$, and $Coma_H$, and the Zernike polynomial rms fit error are given. The total comatic terms include the third, fifth, and seventh order comatic terms.

Wavefront dynamics are affected by signals of the cardiopulmonary system, such as pulse and respiration.[20,21] In particular, this effect is prominent in the lower-order aberrations of defocus and astigmatism.[27] However, changes in comatic terms (both horizontal and vertical) have been shown to be associated with tear film kinetics.[18]

2.3.3 *Lateral shearing interferometer*

In the LSI apparatus,[14,28] the wavefront generated from the HeNe laser illuminates the tear film on the cornea and reflects from its surface. The reflected wavefront is split in the LSI optical wedge into two wavefronts that interfere with each other to create an interferogram. For an evenly spread precorneal tear film, the fringes are regular and horizontal. In the case of an uneven tear film surface, the interference fringes reveal irregularities, and their background is inhomogeneous.[29] The central part of the cornea is exposed to the laser light, thus the tear film in the pupil area (approximately 4×4-mm square region) is measured.

Assessing tear film surface quality from interferometric images is based on estimates of the first harmonic of the interference fringes.[14] The technique combines the traditional spectral estimation techniques with morphological image processing techniques,[23] in which a smoothed 2-D periodogram [fast Fourier transform (FFT)-based spectral estimator] is treated like an image, from which local maxima are extracted

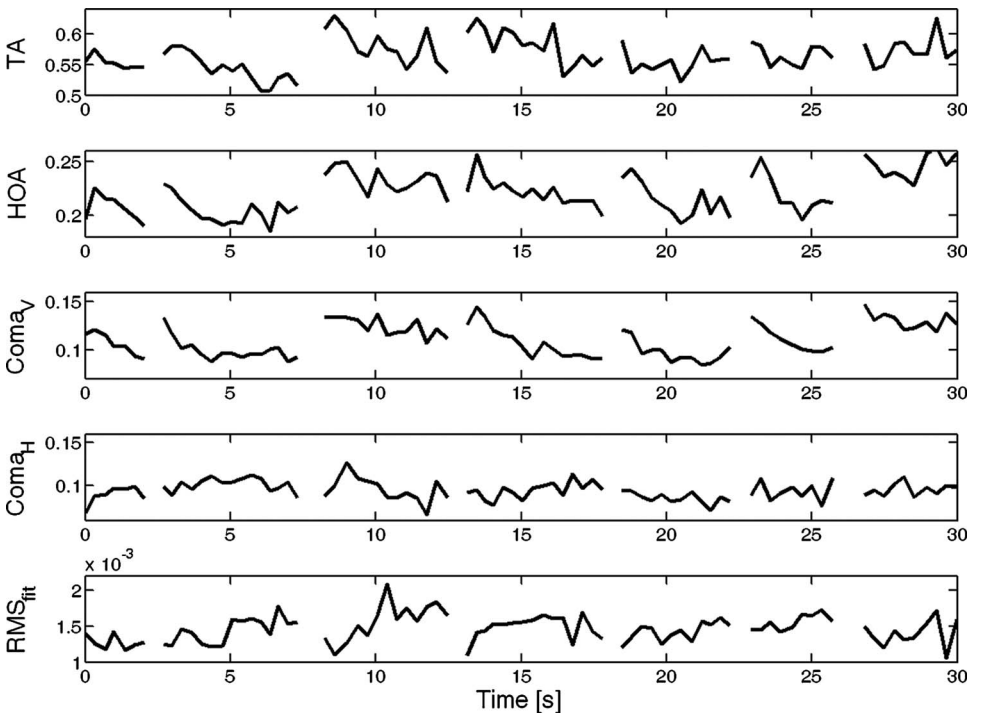

Fig. 3 Examples of the wavefront aberration dynamics (values are in microns). From top to bottom: total wavefront aberrations (excluding piston and prisms), higher-order aberrations, total vertical coma, total horizontal coma, and the Zernike polynomial rms fit error. Gaps in the records indicate the location of blinks that were removed from the dataset.

and classified according to a set of criteria. Finally, a spatial-average localized-weighted estimate of the first harmonic is used as a measure, called M2, of tear film surface quality. An example of the tear film surface quality recorded with the LSI is shown in Fig. 4. The data show the kinetics of the tear film surface after every blink recorded during the sequence. Immediately after each blink, the tear film stabilizes and reveals irregularities. The values of the TFSQ descriptor are high (worse quality) at the beginning, but decrease (better quality) with the tear film build-up time. It has previously been shown that the interferometric method is able to clearly observe the phenomenon of the tear film build-up immediately after each blink.[29]

2.4 *Blinking Patterns*

Each of the three considered techniques for noninvasive measurement of tear film surface quality are based on different physical principles, have a different illumination source, and involve a different subject-instrument interface (i.e., headrest, proximity to instrument's elements, fixation target). Hence, in the initial part of the study, it was important to determine whether the blinking patterns naturally exhibited by subjects changed from one instrument to another.

The group mean interblink interval (mean $\pm$ SD) across the instruments was 3.54 ± 2.52, 2.78 ± 2.48, and 3.18 ± 1.73 sec for HSV, DWS, and the LSI, respectively. Statistical testing by means of the repeated measures ANOVA revealed that across the individual subjects, there were statistically significant differences ($p < 0.05$) in the interblink interval. However, the type of instrument that was used did not cause statistically significant differences ($p > 0.05$). Also, no statistically significant differences were identified when comparing the first 30-sec measurement to the second measurement, indicating that the subjects' blinking patterns were similar in the two consecutive measurements with each of the instruments. The lower sampling rate in DWS (7.5 Hz) as compared to that of HSV and LSI (25 Hz) had little effect on the estimated variability of blink patterns.

2.5 *Tear Film Parameter Estimation*

The time series of a tear film surface quality indicator within an individual interblink interval is used to estimate two pa-

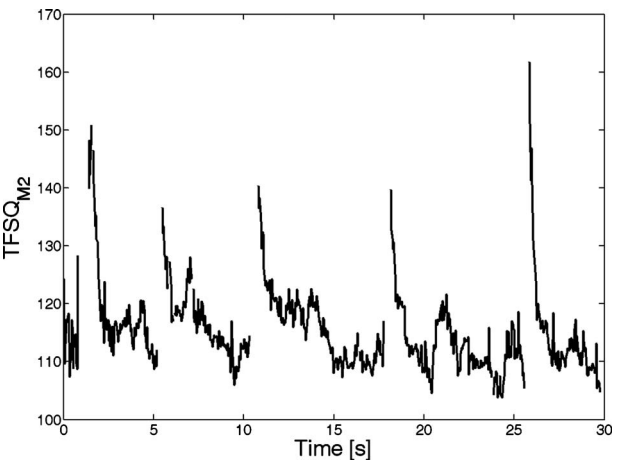

Fig. 4 An example of the tear film surface quality recorded with LSI. Gaps in the record indicate the location of blinks that were removed from the dataset.

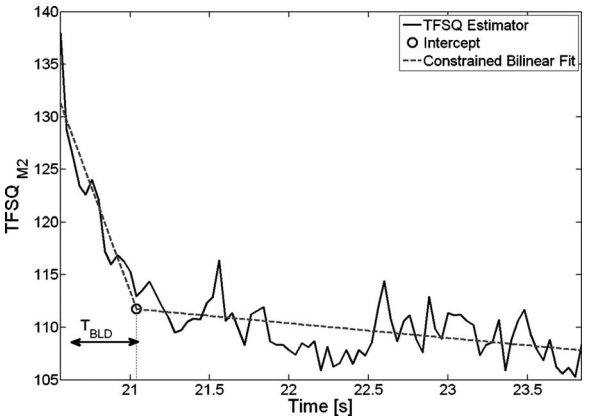

Fig. 5 An example of the estimated tear film surface quality in an interblink interval with a constrained bilinear fit. The intercept of the two linear functions is the estimator of the tear film build-up time T_{BLD}. The estimator $TFSQ_{Av}$ corresponds to the average of TFSQ taken from the intercept to the end of the interblink interval.

rameters: the tear film build-up time T_{BLD}, and the average tear film surface quality $TFSQ_{Av}$, in the stable phase of the interblink interval. This phase is defined as a period from the end of the tear film build-up phase to the end of the interblink interval. Statistical modeling of tear film surface quality has been considered earlier in the context of interferometric data,[30] where a set of four parametric functions has been considered: a bilinear, a trilinear, Hoerl's, and an optimal polynomial function.

The bilinear function seems to be appropriate for the analysis of tear film surface quality in interblink intervals for subjects with normal tears, as they usually exhibit up to two phases of the tear film kinetics (i.e., the tear film build-up phase and the relatively stable interblink phase). In this work, we have extended the bilinear function model so that the second linear function describing the stable interblink phase is constrained by the estimator of the first linear function describing the tear film build-up phase. This is performed using an iterative nonlinear constrained least-squares approach. An example of such bilinear fitting is shown in Fig. 5.

Since the two distinct phases of tear film behavior cannot always be observed in all measured interblink intervals, it was necessary to test in each sequence whether a bilinear fit is warranted. This has been achieved by performing a log likelihood ratio test of the Pearson's correlation coefficients for a linear and bilinear fit, as suggested by Owsley, Knoblauch, and Katholi.[31] In summary, the estimated Pearson's correlation coefficients r_{Lin} and r_{BiLin} are first transformed using Fisher transformation and are multiplied by a factor $\sqrt{N-3}$, with N being the number of sample points, to become standard normal z_{Lin} and z_{BiLin}. Then the log likelihood ratio $-2\log[f(z_{Lin})/f(z_{BiLin})]$, where $f(z)$ denotes the standard Gaussian probability density function, and is χ^2 distributed with 2 deg of freedom. The p-value for which the linear fit was rejected in this test was set to $p<0.01$.

3 Results

3.1 *Tear Film Build-Up Time*

The group statistics of the tear film build-up time measures T_{BLD}, acquired from the three considered instruments, are shown in Table 2. Since the data did not always follow a Gaussian distribution, we also considered the median and the median absolute deviation (MAD).

For the HSV, the group average T_{BLD} was 1.14 sec when calculated across the whole visible corneal surface (AOA) and was 0.99 sec in the pupil area, while the group median values were 0.60 to 0.66 sec, respectively. Five descriptors of T_{BLD} were used in the case of the DWS method. They were based on total aberrations (TA), higher-order aberrations (HOA), total vertical coma ($Coma_V$), total horizontal coma ($Coma_H$), and the Zernike polynomial rms fit error. An increased variability of tear film surface parameter estimates is apparent in the results from the DWS. The group average T_{BLD} ranged from 1.57 sec for vertical coma to 2.46 sec for horizontal coma. Median-based statistics did not reduce the variability,

Table 2 Group statistics of the tear film build-up time across the instruments.

	T_{BLD} (seconds)					
	Count (%)		Mean	Std	Median	MAD
HSV	15	AOA	1.14	1.07	0.60	0.32
	24	Pupil	0.99	0.92	0.66	0.34
DWS	59	TA	1.91	1.85	1.46	0.94
	48	HOA	1.72	2.10	0.77	0.50
	50	$Coma_V$	1.57	1.73	0.75	0.48
	27	$Coma_H$	2.46	2.17	1.92	1.10
	24	rms_{fit}	1.63	1.39	1.10	0.83
LSI	98	M2	0.89	0.74	0.72	0.40

Table 3 Group statistics of $TFSQ_{Av}$ acquired from HSV.

	$TFSQ_{Av}$ from HSV	
	AOA	Pupil
Mean	0.91	0.93
Std	0.02	0.02
Median	0.91	0.94
MAD	0.01	0.01

but rather shifted it toward shorter values (i.e., ranged from 0.75 to 1.92 sec). The group average of the T_{BLD} measure acquired from LSI was 0.89 sec. It is worth noting that the estimated median values for HSV in the pupil area and for vertical coma in DWS are remarkably close to the estimates of median T_{BLD} from LSI.

To ascertain whether the two distinct phases of tear film behavior—the build-up phase and the stability phase—were observed in all measured interblink intervals, a count was kept on how many times the hypothesis of a single linear fit (rather than the bilinear fit) to the interblink data was rejected. The number of rejected linear fits to the data was on average 20, 42, and 98% of the total number of interblink intervals for the HSV, DWS, and the LSI, respectively (see the percentage count in Table 2). This indicates that the phase of tear film build-up was almost always observed with the LSI technique, but not using the HSV and DWS methods. No cases were encountered in which the hypothesis of the linear fit to the data was retained for all interblink intervals in the measurement.

3.2 *Tear Film Surface Quality*

The statistics of the average tear film surface quality in the stable phase of the interblink interval $TFSQ_{Av}$, acquired from HSV using the entire visible corneal area (AOA) and the pupil area, are shown in Table 3. The estimated averages and standard deviations are very close to median and MAD values, indicating only small numbers of outliers. We note that the tear film quality within the pupil is, as expected, slightly better than across the whole area of analysis.

The statistics of the tear film parameters acquired from DWS are shown in Table 4. Large variations were observed between the mean/standard deviation and median/MAD statistics only for $TFSQ_{Av}$ based on total aberrations.

Table 5 Group statistics of $TFSQ_{Av}$ acquired from LSI.

	$TFSQ_{Av}$ from LSI
Mean	112.04
Std	7.69
Median	111.14
MAD	5.04

The statistics of the tear film parameters acquired from LSI are shown in Table 5. As in the case of the HSV technique, there was not much difference between the mean/standard deviation and median/MAD statistics.

The mean and median values for the estimator of $TFSQ_{Av}$ are similar, indicating that the data are not skewed and are free of outliers. This is not the case for the estimator of T_{BLD}, where median values were consistently lower than the mean values. One possible explanation is the observed nature of the build-up phase that occasionally exhibits longer periods of tear film formation, and hence does not follow a Gaussian distribution.

3.3 *Instrument Precision*

To ascertain the precision of the instrument in measuring $TFSQ_{Av}$, the coefficient of variation CV was also calculated. First, the coefficient of variation was calculated using the original TFSQ data in the stable phase of the interblink interval. This was followed by calculating the coefficient of variation for detrended data, in which the linear trend in TFSQ was removed. The group statistics of the coefficient of variation for the $TFSQ_{Av}$ are given in Table 6.

The coefficient of variation for $TFSQ_{Av}$ in HSV was found to be very low (below 1%). The precision of the DWS in quantifying tear film surface quality was found to be more variable. The coefficient of variation for $TFSQ_{Av}$ ranged from about 1.5% for the total aberrations to about 15% for the horizontal coma, when the linear trend in the TFSQ was removed. This result was expected, as the total aberrations, which are dominated by the spherical and cylindrical compo-

Table 4 Group statistics of $TFSQ_{Av}$ acquired from DWS.

	$TFSQ_{Av}$ from DWS				
	TA (μm)	HOA (μm)	$Coma_V$ (μm)	$Coma_H$ (μm)	RMS_{fit} (nm)
Mean	1.50	0.23	0.10	0.09	1.00
Std	1.40	0.10	0.07	0.06	0.30
Median	1.10	0.22	0.10	0.07	1.00
MAD	0.52	0.06	0.03	0.04	0.20

Table 6 Group statistics of the coefficient of variation (CV) across the instruments.

		CV(%)		CV(%) (detrended)	
		Mean	Std	Mean	Std
HSV	AOA	0.66	0.25	0.58	0.22
	Pupil	0.57	0.32	0.51	0.25
DWS	TA	2.96	3.11	1.47	1.35
	HOA	5.88	4.48	4.16	3.00
	$Coma_V$	11.81	6.82	8.26	4.92
	$Coma_H$	22.70	16.35	14.43	10.32
	rms_{fit}	11.78	5.40	8.26	4.05
LSI	M2	3.95	1.58	2.84	1.01

nents, are usually more stable than the higher-order aberrations. The coefficient of variation for $TFSQ_{Av}$ for the LSI method was also found to be low at 3%.

3.4 *Correlation between Instruments*

Pearson's r^2 coefficient was calculated to ascertain the correlation between T_{BLD} and $TFSQ_{Av}$ measured with each pair of the three considered instruments. The results are shown in Tables 7 and 8.

Moderate but significant correlation was found between T_{BLD} measured with LSI and DWS based on the vertical coma ($r^2=0.34$, $p<0.01$), and between LSI and DWS ($r^2=0.31$, $p<0.01$) based on the high-order aberrations. Also, moderate but significant correlation was found between $TFSQ_{Av}$ measured with LSI and HSV ($r^2=0.35$, $p<0.01$) and between LSI and DWS ($r^2=0.40$, $p<0.01$) based on the rms fit error. No significant correlation was found between HSV and DWS for both T_{BLD} and $TFSQ_{Av}$.

Statistical significance testing by means of the repeated measures ANOVA for each of the instruments revealed that across the subjects, there are statistically significant differences ($p<0.05$) in T_{BLD} and $TFSQ_{Av}$, suggesting that the tear film build-up process as well as the tear film quality level are different between subjects. However, for each of the methods, no statistically significant differences were found in $TFSQ_{Av}$ for an individual subject, across the interblink intervals (within a 30-sec measurement period), or between the two sequential 30-sec measurement periods. Considering the T_{BLD} computed for pairwise comparison across instruments, no statistically significant differences were observed between the HSV and LSI ($p>0.05$), while DWS showed statistically significant differences when compared to the other two instruments. Hence, as expected from the descriptive statistics, HSV and LSI provide close agreement for measurements of T_{BLD}, while DWS differs from the HSV and LSI results.

4 Discussion

We have compared three instruments for noninvasive assessment of tear film surface quality (TFSQ), in terms of their precision and agreement for measurements describing the characteristics of the kinetics of the tear film in normal subjects. We aimed to ascertain whether each of the three techniques—the dynamic-area HSV, dynamic wavefront sensing (DWS), and lateral shearing interferometry (LSI)—were capable of consistently and reliably evaluating the quality of tear film surface in natural blinking conditions. It was also of interest whether the estimates of tear film surface quality pa-

Table 7 Correlation between T_{BLD} measured with the three instruments. The asterisk indicates statistically significant values ($p<0.01$).

Pearson's correlation coefficient						
		DWS				
	LSI	TA	HOA	$Coma_V$	$Coma_H$	rms_{fit}
HSV (pupil)	0.05	0.00	0.02	0.01	0.00	0.16
LSI	—	0.09	0.31*	0.34*	0.05	0.01

Table 8 Correlation between $TFSQ_{Av}$ measured with the three instruments. The asterisk indicates statistically significant values ($p<0.01$).

Pearson's correlation coefficient						
		DWS				
	LSI	TA	HOA	$Coma_V$	$Coma_H$	rms_{fit}
HSV (pupil)	0.35*	0.03	0.02	0.03	0.07	0.04
LSI	—	0.01	0.00	0.01	0.00	0.40*

rameters, such as the tear film build-up time and the average tear film surface quality in the stable phase of the interblink interval, were comparable between the instruments.

Since each of the three considered techniques are based on different physical principles, and since the TFSQ descriptors could not be normalized, it was not possible to directly compare the results of average TFSQ from one instrument with the other. The size and location of the area of analysis in each of the instruments were different, so the pupil areas that were used in each of the instruments were only approximately equal. Also worth noting are the spatial sampling differences between the instruments. The DWS technique samples the pupil area at about 210-μm intervals. The rings in HSV are spaced between 150 and 180 μm, while its angular resolution is determined by the charge-couple device (CCD) pixel size. Finally, the LSI technique has a resolution of 140 pixels per mm (7-μm interval). Nevertheless, Pearson's correlation analysis revealed that the LSI technique was providing $TFSQ_{Av}$ that moderately but statistically significantly correlated with the measurement obtained with HSV and DWS, while this was not the case when the HSV technique was compared to DWS. A reason for this could be some difference in the area of the analysis used in both techniques, as the pupil size in HSV measurement is normally smaller than that measured in DWS. The three instruments were found to differ in their precision for deriving the average TFSQ, with the HSV instrument found to be the most precise (i.e., lowest CV), and measures derived from the DWS were typically found to have the lowest precision (i.e., highest CV).

The tear film build-up time is potentially a useful descriptor of tear film dynamics,[5,16] and it can be compared directly between the instruments. This parameter essentially represents the time required following a blink for the tear film quality to stabilize. For all considered instruments, the estimated tear film build-up time was less than 2.5 sec and showed a remarkably close median value of around 0.7 sec. This suggests that the tear film reaches stable levels relatively rapidly following a blink in normal subjects. This rapid stabilization of the tear film following a blink is advantageous for the visual system, as it ensures a stable optical surface of the anterior eye throughout the majority of the interblink interval. Our findings are in contrast to some previous results recorded with videokeratoscopy[5,6] and wavefront sensing,[12] where values of tear film build-up time from 4 to 7 sec were recorded. Differences in the analysis techniques employed, the sampling frequency of the instruments, and the measurement protocols utilized are the likely reasons for the differences noted with these previous studies. In particular, those studies used a protocol in which subjects were asked to blink to try to keep their eyes open, rather than blinking naturally. Our findings do agree closely with those of Szczesna and Kasprzak[29] utilizing LSI on a different group of subjects, and with Owens and Philips,[32] who estimated the velocity of the particles in the tear film and the time to tear stabilization of 1.05 ± 0.3 sec. Our results are also consistent with previous estimates of the tear film lipid layer spread of Goto and Tseng[33] (0.36 ± 0.22 sec) and Yokoi et al.[16] (less than 0.5 sec), who used another interferometric technique (DR-1 camera), and of Zhu, Collins, and Iskander,[18] who measured postblink changes in corneal topography and estimated tear film build-up time to be less than 1 sec. The improvement of tear film surface quality during the build-up phase, as its name could suggest, may not necessarily be associated with the thickening of tear film, but most likely with the increase of tear film smoothness.[34,35] Hence, the tear film smoothing phase can seem to be a more appropriate name for this phase of tear film dynamic.

We found that the DWS system exhibited lower precision in terms of the average tear film surface quality, and had less agreement in terms of tear film build-up time. In contrast to HSV and LSI, the DWS provides dynamic information regarding changes in the optical quality of the whole eye (as opposed to the dynamics of the anterior surface of the eye alone, as provided by HSV and LSI), and as such can be influenced by concomitant changes in other ocular structures not related to the tear film. Changes in aberrations due to nontear-film-related ocular components (e.g., lens fluctuations or retinal movement) is the likely reason for the lower precision and differences found in tear film build-up time with DWS. There was no significant difference found between measurements obtained using total wavefront aberrations and higher-order aberrations, suggesting that the influence of the cardiopulmonary signals on the lower-order aberrations are of little significance in the measurement of tear film surface quality. The Zernike polynomial rms fit error that has been advocated as a descriptor for tear film surface quality[7,25] showed better performance than the other considered measures based on wavefront aberrations, and was the only DWS parameter to show a moderate correlation with the LSI technique.

In conclusion, the technique of dynamic-area HSV was the most precise method for measuring the average TFSQ by virtue of its lower coefficient variation. It was closely followed by LSI, which also showed low variability within the inter-

blink interval. The LSI technique also appears to be the most sensitive technique for measuring the changes in the tear film surface associated with the tear film build-up phase. We found that the tear film build-up (smoothing) phase is consistently present in natural blinking, but it requires very sensitive methods for its detection. Although in general, the DWS system exhibited lower precision in terms of the average tear film surface quality, and less agreement in terms of tear film build-up time, moderate but significant correlation has been found between estimates of T_{BLD} using $Coma_V$ and HOA descriptors and estimates using LSI. This indicates that DWS also has potential for describing tear film kinetics. Therefore, whilse HSV and LSI techniques demonstrated superior precision to the DWS technique, all three techniques appear to exhibit some merit for describing aspects of the quality and dynamics of tear film. The fact that the techniques are based on different physical principles and have slightly different measurement/analysis areas on the ocular surface suggests that the three techniques can provide information regarding slightly different aspects of the tear film. This study has established the relative precision and reliability of these noninvasive techniques for tear film assessment in normal subjects: however, further information regarding the techniques will be provided by future research investigating the abilities of the methods to detect dry eye, and differentiate dry eye from normal tear film quality.

Acknowledgments

Part of this study was funded by the 2008 Endeavour Research Fellowship, ERF08_PDR_884, to Dorota H. Szczesna. We thank Beata Sander for assistance with the clinical examination of subjects participating in the study.

References

1. K. K. Nichols, G. L. Mitchell, and K. Zadnik, "The repeatability of clinical measurements of dry eye," *Cornea* **23**(3), 272–285 (2004).
2. DEWS, "Methodologies to diagnose and monitor dry eye disease: report of the Diagnostic Methodology Subcommittee of the International Dry Eye Work-Shop (2007)," *Ocul. Surf.* **5**, 108–152 (2007).
3. L. S. Mengher, A. J. Bron, S. R. Tonge, and D. J. Gilbert, "A non-invasive instrument for clinical assessment of the pre-corneal tear film stability," *Curr. Eye Res.* **4**(1), 1–7 (1985).
4. J. P. Guillon, "Non-invasive tearscope plus routine for contact lens fitting," *Cont. Lens Anterior Eye* **21**(Supp. 1), S31–S40 (1998).
5. J. Nemeth, B. Erdélyi, B. Csákány, P. Gáspár, A. Soumelidis, F. Kahlesz, and Z. Lang, "High-speed videotopographic measurement of tear film build-up time," *Invest. Ophthalmol. Visual Sci.* **43**(6), 1783–1790 (2002).
6. R. Montés-Micó, J. L. Alió, G. Muñoz, and W. N. Charman, "Temporal changes in optical quality of air-tear film interface at anterior cornea after blink," *Invest. Ophthalmol. Visual Sci.* **45**(6), 1752–1757 (2004).
7. D. R. Iskander, M. J. Collins, and B. Davis, "Evaluating tear film stability in the human eye with high-speed videokeratoscopy," *IEEE Trans. Biomed. Eng.* **52**(11), 1939–1949 (2005).
8. M. Kopf, Y. Fan, D. R. Iskander, A. J. Shaw, and B. Straker, "Tear film surface quality with soft contact lenses using dynamic videokeratoscopy," *J. Optometry* **1**(1), 14–21 (2008).
9. L. N. Thibos and X. Hong, "Clinical applications of the Shack-Hartmann aberrometer," *Optom. Vision Sci.* **76**(12), 817–825 (1999).
10. N. L. Himebaugh, L. N. Thibos, A. Bradley, G. Wilson, and C. G. Begley, "Predicting optical effects of tear film break up on retinal image quality using the Shack-Hartmann aberrometer and computational optical modeling," *Adv. Exp. Med. Biol.* **506**(Pt B), 1141–1147 (2002).
11. S. Koh, N. Maeda, T. Kuroda, Y. Hori, H. Watanabe, T. Fujikado, Y. Tano, Y. Hirohara, and T. Mihashi, "Effect of tear film break-up on higher-order aberrations measured with wavefront sensor," *Am. J. Ophthalmol.* **134**(1), 115–117 (2002).
12. R. Montés-Micó, J. L. Alió, and W. N. Charman, "Postblink changes in the ocular modulation transfer function measured by a double-pass method," *Invest. Ophthalmol. Visual Sci.* **46**(12), 4468–4473 (2005).
13. A. Dubra, C. Paterson, and C. Dainty, "Double lateral shearing interferometer for the quantitative measurement of tear film topography," *Appl. Opt.* **44**(7), 1191–1199 (2005).
14. D. H. Szczesna, J. Jaronski, H. T. Kasprzak, and U. Stenevi, "Interferometric measurements of dynamic changes of tear film," *J. Biomed. Opt.* **11**(3), 34028 (2006).
15. D. H. Szczesna, H. T. Kasprzak, J. Jaronski, A. Rydz, and U. Stenevi, "An interferometric method for the dynamic evaluation of the tear film," *Acta Ophthalmol. Scand.* **85**(2), 202–208 (2007).
16. N. Yokoi, H. Yamada, Y. Mizukusa, A. J. Bron, J. M. Tiffany, T. Kato, and S. Kinoshita, "Rheology of tear film lipid layer spread in normal and aqueous tear-deficient dry eyes," *Invest. Ophthalmol. Visual Sci.* **49**(12), 5319–5324 (2008).
17. P. E. King-Smith, B. A. Fink, J. J. Nichols, K. K. Nichols, R. J. Braun, and G. B. McFadden, "The contribution of lipid layer movement to tear film thinning and breakup," *Invest. Ophthalmol. Visual Sci.* **50**(6), 2747–2756 (2009).
18. M. Zhu, M. J. Collins, and D. R. Iskander, "Dynamics of ocular surface topography," *Eye* **21**(5), 624–632 (2007).
19. D. Alonso-Caneiro, D. R. Iskander, and M. J. Collins, "Assessment of tear film surface quality using dynamic-area high-speed videokeratoscopy," *IEEE Trans. Biomed. Eng.* **56**(5), 1473–1481 (2009).
20. D. R. Iskander, M. J. Collins, M. R. Morelande, and M. Zhu, "Analyzing the dynamic wavefront aberrations in human eye," *IEEE Trans. Biomed. Eng.* **51**(9), 1969–1980 (2004).
21. M. Zhu, M. J. Collins, and D. R. Iskander, "Microfluctuations of wavefront aberrations of the eye," *Ophthalmic Physiol. Opt.* **24**(6), 562–671 (2004).
22. M. A. Lemp, "Report of the national eye institute/industry workshop on clinical trials in dry eyes," *CLAO J.* **21**(4), 221–232 (1995).
23. D. H. Szczesna and D. R. Iskander, "Robust estimation of tear film surface quality in lateral shearing interferometry," *J. Biomed. Opt.* **14**, 064038 (2009).
24. M. H. Hennig and F. Wörgötter, "Eye micro-movements improve stimulus detection beyond the Nyquist limit in the peripheral retina," in *Advances in Neural Information Processing Systems 16*, S. Thrun, L. Saul, and B. Schölkopf, Eds., MIT Press, Cambridge, MA (2004).
25. N. L. Himebaugh, C. G. Begley, Z. Wu, R. L. Chalmers, and K. Moody, "Application of RMS fit error for assessing pre-lens tear film break-up," *Invest. Ophthalmol. Visual Sci.* **50**, E-Abstract 535 (2009).
26. J. Schwiegerling, "Scaling Zernike expansion coefficients to different pupil sizes," *J. Opt. Soc. Am. A* **19**(10), 1937–1945 (2002).
27. M. J. Collins, B. Davis, and J. Wood, "Microfluctuations of steady-state accommodation and the cardiopulmonary system," *Vision Res.* **35**(17), 2491–2502 (1995).
28. D. H. Szczesna, H. T. Kasprzak, and U. Stenevi, "Application of interferometry for evaluation of the effect of contact lens material on tear film quality," *Proc. SPIE* **7064**, 706407 (2008).
29. D. H. Szczesna and H. T. Kasprzak, "Numerical analysis of interferograms for evaluation of tear film build-up time," *Ophthalmic Physiol. Opt.* **29**(3), 211–218 (2009).
30. D. Alonso-Caneiro, D. H. Szczesna, D. R. Iskander, and M. J. Collins, "Context-based modelling of interferometric signals for the assessment of tear-film surface quality," *Proc. IEEE Workshop Stat. Signal Process.*, pp. 553–556, IEEE, Piscataway, NJ (2009).
31. C. Owsley, K. Knoblauch, and C. Katholi, "When does visual aging begin?" *Invest. Ophthalmol. Visual Sci.* **33**(4), 1414 (1992).
32. H. Owens and J. Philips, "Spreading of tears after blink: velocity and stabilization time in healthy eyes," *Cornea* **20**(5), 484–487 (2001).
33. E. Goto and S. C. G. Tseng, "Differentiation of lipid tear deficiency dry eye by kinetic analysis of tear interference images," *Arch. Ophthalmol.* **121**(2), 173–180 (2003).
34. S. I. Brown and D. G. Dervichian, "Hydrodynamics of blinking. In vitro study of the interaction of the superficial oily layer and the tears," *Arch. Ophthalmol.* **82**(4), 541–547 (1969).
35. D. A. Benedetto, T. E. Clinch, and P. R. Laibson, "*In vivo* observation of tear dynamics using fluorophotometry," *Arch. Ophthalmol.* **102**(3), 410–412 (1984).